

Design and Performance Testing of a Parabolic Trough Collector Including Deformation Test of the Receiver Tube

Open
Access

Ali Jaber Abdulhamed^{1,2,*}, Maithem Hussein Rasheed³, Hanaa Kadhim Kareem⁴, Nor Mariah Adam², Mohd Zainal Abidin Ab-Kadir², Abdul Aziz Hairuddin²

- ¹ Automotive Engineering Department, College of Engineering /AL-Musaib, University of Babylon, Hilla, Babylon, Iraq
² Department of Mechanical and Manufacture Engineering, Faculty of Engineering, University Putra Malaysia, 43400 UPM Serdang, Selangor, Malaysia
³ Energy Engineering Department, College of Engineering /AL-Musaib, University of Babylon, Hilla, Babylon, Iraq
⁴ Training Energy Researches Office, Ministry of Electricity, Baghdad, Iraq

ARTICLE INFO

ABSTRACT

Article history:

Received 12 November 2019
Received in revised form 24 December 2019
Accepted 24 December 2019
Available online 18 March 2020

Source of clean drinkable water is a big problem in the world. Water purification processes consume the fuel which extremely effect on environment, economy, and human health. Solar parabolic trough collector (PTC) was built to meet the requirement of drinking water for the village members in desert areas without relying on fossil fuel. The PTC powered by solar energy is the most favourable compared to flat plate because higher temperature is obtained. The design, fabrication, and performance medium-scale of a stainless steel solar-powered parabolic trough collector (PTC) with a 90° rim angle and 3 m×1.314 m aperture area as a hot water generating system were investigated in this paper. Theoretical calculations and primary design were achieved with all possible evaluations that provide accuracy design able to produce 200 L/day of water with more than 80°C. A certain amount of load equal to the force generated by 34 m/s wind blowing was applied to the PTC and deformed the parabola within acceptable limits. The gravity-load- and thermal-expansion-induced deformation of the receiver tube was also investigated. Comparing such deformation with the width of the solar image in the focal plane revealed a maximum deformation of 1.43 mm in the mid length of the receiver tube that was within acceptable limits. The deformation of the receiver tube is an important new test to assess the thermal performance of PTC. The performance of PTC was assessed based on the ASHRAE Standard 93. The reflected energy distribution of parabolic surface errors showed a standard deviation of 0.009165 rad, which, according to ASHRAE Standard 93, indicates that the parabolic surface has a high reliability. The collector time constant was set to 75 s, while the slope and intercept tests of the collector efficiency equation were 0.2358 and 0.72987, respectively. The experimental results show that the maximum water obtained from system is more than 226 L/day with temperature $\geq 50^\circ\text{C}$ at flow rate of 0.00925 kg/s, and at mentioned flow rate is 92°C.

Keywords:

parabolic trough collector; receiver deformation; wind load test; performance characteristics; collector time constant; hot water generation

Copyright © 2020 PENERBIT AKADEMIA BARU - All rights reserved

* Corresponding author.

E-mail address: alijaberabdulhamed@gmail.com (Ali Jaber Abdulhamed)

1. Introduction

Energy demand has been increasing with the population and the rising standard of living. The use of unclean energy sources adversely affects the economy, the environment, and human health. Therefore, many countries prefer to use renewable energy sources, such as wind and solar energy, to fulfill their energy requirements without depending on fossil fuels [1-3]. Solar energy is one of the most promising renewable energy sources available at present. Among different types of solar collectors, the parabolic trough collector (PTC) has been receiving considerable attention for a wide range of applications, particularly in hot water production [1, 4-5] and industrial steam generation Thomas [6-7]. PTCs are preferred for solar steam generation due to their capability to attain a temperature of 400 °C [2, 8].

A PTC is a promising solar collector technology that converts solar irradiation into thermal energy by collecting solar incident rays from the sun and then reflecting them onto a linear receiver tube that contains a heat transfer fluid (HTF) to produce heat [3, 9-10]. The accuracy of a parabolic surface is a crucial factor that affects the efficiency and performance of a PTC. PTC design should consider the capability of a PTC to carry its own weight and resist wind force. The accuracy of a parabolic trough surface is evaluated through a collector performance test according to the American Society of Heating, Refrigerating, and Air-Conditioning Engineers (ASHRAE) Standard 93 (1986; a test method for determining the thermal performance of solar collectors) Valan and Sornakumar [11].

Jaramillo *et al.*, [12] designed, constructed, evaluated, and tested five aluminum solar PTCs for hot water generation. Two of them were designed with a 45° rim angle and the other three with a 90° rim angle. The thermal test for both designs was determined based on the Standard ASHRAE 93-1986. Maximum efficiency was calculated for collectors with a rim angle of 90° is 67%, whereas maximum efficiency achieved for solar collectors with a rim angle of 45° is 35% [12].

Several researchers [2,13-14] present comprehensive reviews of previous works on PTC performance improvement with novel receiver geometries including corrugated pipes [15-16], converging-diverging pipes [17], dimpled pipe [18], longitudinal vortex generators [19], helical fins [20], metal foam [21], porous discs [22], perforated plate inserts [23], conical inserts [24], twisted tape inserts [25-26], and wavy pipes [27]. Comprehensive description and review of the aforesaid and additional receiver arrangements are mentioned in References [13,28] and are not discussed further hither for brevity. Previous reviews discuss the variety of receiver geometries and improvement the overall collector performance by inducing turbulence for an enhanced mixing or increasing the heat transfer surface area with additional heat flow. However, literature review indicates that a deformation of receiver tube has not been studied yet.

The design, fabrication, and performance of a solar-powered parabolic trough collector (PTC) as a hot water generating system were investigated in this paper. This collector comprises a parabola-shaped reflective material (stainless steel), receiver tube, and support structures with manual tracking. The deformation of the receiver tube was also tested as a new important exam to assess the thermal performance of PTC.

2. Methodology of PTC Design

In designing a PTC system, the parabolic curve should be carefully considered to ensure that most incident radiation will be reflected to the focal point. The construction accuracy of a PTC surface is evaluated according to ASHRAE Standard 93 (1986) ASHRAE [29].

According to dimensions that obtained from Eq. (2) and Eq. (3) with 90° of rim angle (ϕ_r), one rib model was fabricate as a template for the second piece. The rib width, depth and thickness that calculated from equations were 132.4 cm 32.8 cm and 2 cm respectively, as shown in Figure 3

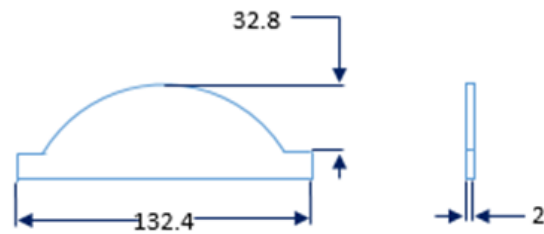


Fig. 3. Parabolic rib (all dimensions are in cm)

Then, the two ribs are connected using five straight hollow square tubes with length of 3m to produce PTC structure as presented in Figure 4.



Fig. 4. Parabolic trough structure

A stainless-steel plate with a thickness of 1 mm was fixed with four bolts over the parabolic trough structure as shown in Figure 5.



Fig. 5. Parabolic trough structure with plate

Then, the support structure with manual tracking which consist of three parts was built. This structure enables the system to manually track the movement of the sun in two axis, as shown in Figure 6(a), (b) and (c).

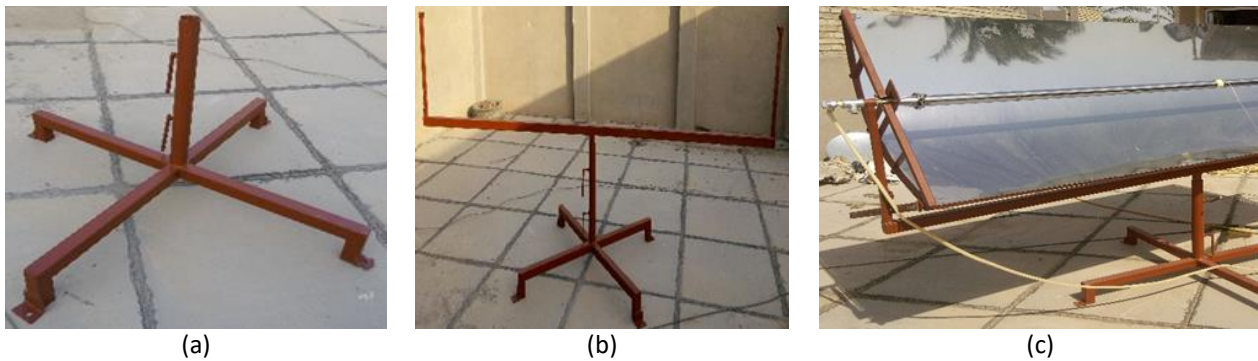


Fig. 6. Stages manufacture of PTC system. (a). first part of support structure, (b). assemble first and second part of support structure with allow movement to left and right, (c). assemble three part of support structure with movement in two axis

3. Result and Discussions

3.1 Load Testing

Gravity and wind loads are torque loads that affect PTCs. Gravity load is produced when the centre of gravity is not centred with the axis. Wind load on the trough was calculated using sand to simulate the load. Sand was measured with a weight balance machine before it was loaded into the trough. Sand was added gradually to the trough, which was maintained in a horizontal position. A dial gauge (Figure 7(a)) was placed below the stainless-steel parabolic trough to measure deflection, as shown in Figure 7(b).



Fig. 7. (a) dial gauge, (b) PTC with dial gauge

The maximum weight of the sand added to the trough was 72 kg, which represented a wind velocity of 34 m/s. A wind force of 72 kg for the design wind velocity of 34 m/s was estimated for the parabolic trough in the work of Randall (1981) by using the method prescribed in “the code of practice for design loads for buildings and structures” IS: 875–Part 3 (1987) Valan and Sornakumar [11]. It is worth noting that the maximum wind velocity recorded in Julay and August 2019 where the system tested was 34 m/s [34].

The experimental test showed that the deflection at the center of the parabolic trough with a full load was only 0.86 mm, which is within acceptable limits. The load starts exerting an effect after a weight of 15 kg is reached, as shown in Figure 8.

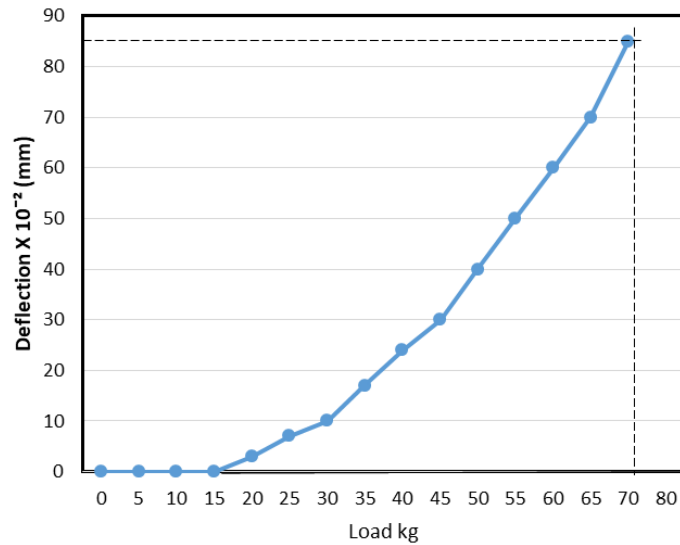


Fig. 8. Deflection versus load

3.2 System Description

The solar-powered PTC system is utilized to generate hot water. The system consists of a PTC, a hot water accumulative tank, and a cold water source. The length of system (parabolic collector or receiver tube) is limited according to available space, then according literature review the optimum rim angle is 90°. The parabola built according to the characteristics and dimensions of the newly developed PTC that obtained from theoretical equations from Eqs. (1) to (3) are provided in Table 1. The PTC comprises a flexible material for the solar reflector with a reflectance of 0.947. The receiver tube which placed in a focal line at distance of 32.8 cm, was fabricated from a stainless-steel material. Water from the cold water source flows through the stainless steel tube, where it is heated, and then it flows back into the hot water accumulative tank. The dimensions of stainless-steel tube were estimated from receiver tube designed in previous work for authors as listed in Table 1 [34].

Table 1

The dimensions of parabola trough with receiver tube

Description	Dimensions
Parabola length (L)	300 (cm)
Parabola aperture (W_a)	131.4 (cm)
Focal distance (f)	32.8 (cm)
Rim angle (ϕ_r)	90°
Thickness of parabolic steel plate	1 (mm)
Inside receiver tube diameter (D_i)	50 (mm)
Outside receiver tube diameter (D_o)	51 (mm)
Parabola height (h_p)	32.8 (cm)

The PTC rotates manually in two axes to track the sun as it moves across the sky during the day. Type K thermocouple wires and readers were used to record the temperature in the inlet (T_{in}) and the outlet (T_{out}) of the receiver tube. The experiments were conducted on various days from 8:00

a.m. to 5:00 p.m. in Baghdad, Iraq with a mean solar beam radiation (I_b) within the range of 1800–2200 W/m^2 and a mean ambient temperature ($T_{amb.}$) within the range of 45°C–52°C. The maximum hot water at the receiver outlet was measured as 82 °C.

3.3 Deformation of the Receiver Tube (δ_R)

The deflection of the receiver tube was compared with the width of the solar image in the focal plane. To guarantee non-disparity, the width of the solar image must be larger than the diameter of the receiver tube. Otherwise, the radiation reflected on the receiver tube will be poorly distributed, thereby reducing the thermal efficiency of the PTC.

As shown in Figure 2, the width of the focal zone was measured based on the radiation reflected from the rim of the parabola. The width of the solar image in the focal plane increases along with the rim angle. The solar radiation incident beam has a cone shape with an angular width of $2\varphi = 0.53^\circ$ and half-angle (φ) width of 0.267° . The incident beam is radiated on the concentrator at a direction parallel to the central plane of the parabola [35-36].

Solar radiation falls on the solar reflector at point B, the angle (AFB) represent the rim angle (φ_r) and was used to estimate the maximum mirror radius (r_r) as shown in Figure 2.

The diameter of a semicircular receiver (Figure 2) can represent the width (w) of the flat receiver on the focal plane of the parabola. This width can be defined as R_{abl} [36]

$$w = \frac{W_a \sin 0.267}{\sin \varphi_r \cos(\varphi_r + 0.267)} \quad (4)$$

Based on this equation, w is equal to 56.4 mm. As shown in Figure 9, the deflection of the receiver was measured by placing a dial gauge in the mid length of the receiver tube on which the highest deformation was observed.



Fig. 9. Dial gauge on the mid length of the receiver tube

Four tests were performed on a (1) plain tube, (2) a plain tube with full load water flow, (3) a tube with insert rings, and (4) a tube with insert rings and full load water flow to estimate the extent of deformation of the receiver tube. The loads applied in (2) and (4) were 8.75 kg and 10.5 kg, respectively. A weight balance machine was used to measure the load of the receiver tube before installing this tube into a PTC. The thermal-expansion-induced deformation was measured at 30-minute intervals. As shown in Figure 10, a maximum deformation of 1.43 mm was recorded in (2).

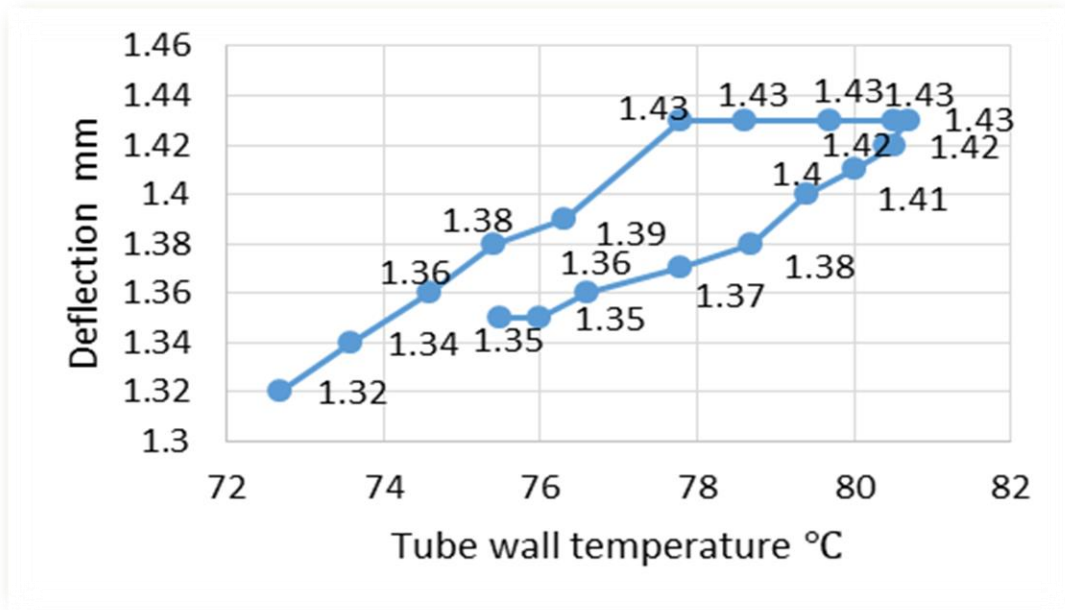


Fig. 10. Deflection of the receiver plain tube against the tube wall temperature

Meanwhile, as shown in Figure 11, a maximum deformation of 1.13 mm was recorded in (4). Given that using insert rings in (3) and (4) can support the tube, therefore, the maximum deformation in (1) was higher than that in (3).

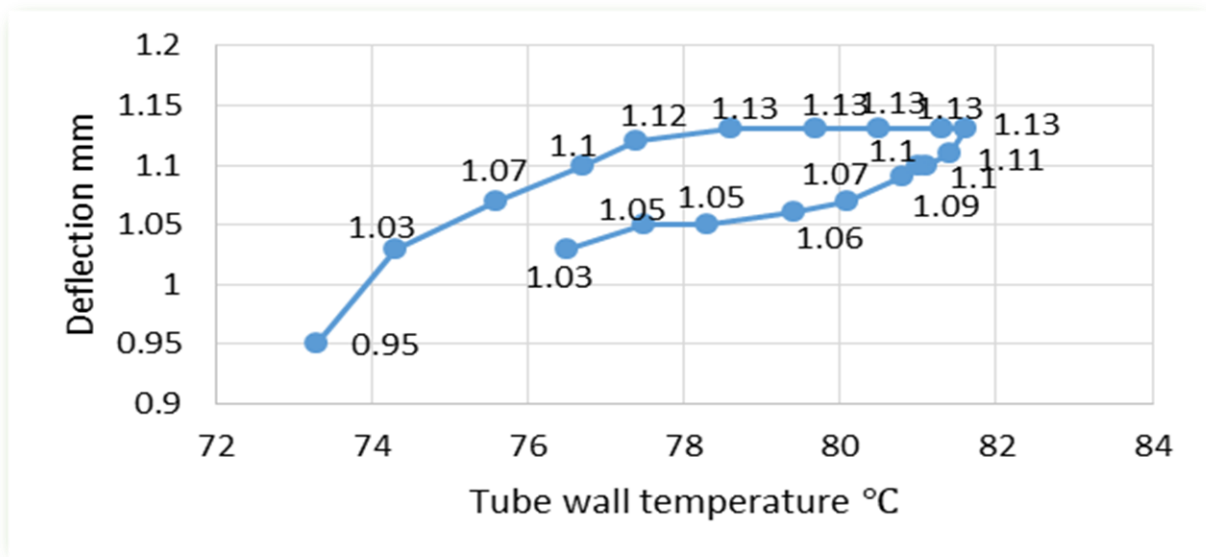


Fig. 11. Deflection of the receiver tube equipped with insert rings against the tube wall temperature

A 1.43 mm maximum deformation was recorded in the mid length of the receiver tube and was attributed to both gravity load and thermal expansion. As shown in Figure 12, this deformation is within acceptable limits when compared with the width of the solar image in the focal plane.

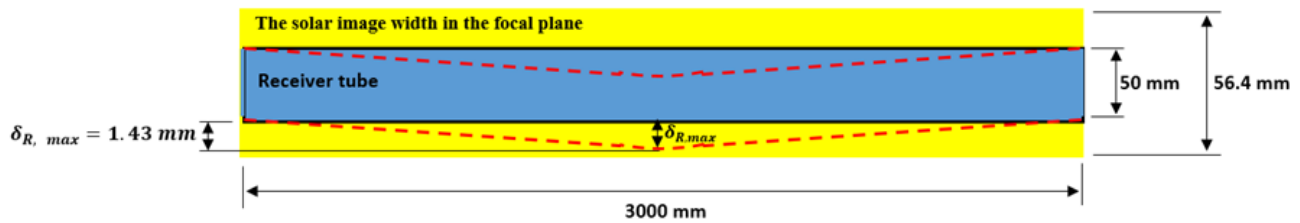


Fig. 12. Deformation of the receiver tube

3.4 Parabolic Surface Error

The parabolic surface should be carefully constructed because it affects the shape and direction of the reflecting surface. Parabolic surface errors have two types: random and nonrandom [19, 20]. The former is modeled statistically by the standard deviations of the total reflected energy distribution at normal incidence (σ_{total}), which is expressed as [30, 38]

$$\sigma_{total} = \sqrt{\sigma_{sun}^2 + 4\sigma_{slope}^2 + \sigma_{mirror}^2} \quad (5)$$

The deformation of the parabola (σ_{slope}), which occurs as a result of wind loading random error, is the most important because the (σ_{slope}) term in Eq. (5) is multiplied by a factor of 4. Therefore, considerable caution should be taken when building the parabolic surface. Treadwell (1976) explained that tracking and slope errors are less evident with a 90° rim angle because the mean focus to reflector distance, and consequently, the reflected beam spread, is minimized Treadwell [39]. Accordingly, the current work considered a rim angle of 90°. The parabolic surface error is 0.009165 rad according to ASHRAE Standard 93 (1986); this value indicates that the surface is accurately built.

Nonrandom errors appear during PTC assembly, fabrication, or operation. They can be identified as reflector profile, receiver location, and misalignment errors via physical measurement Güven and Richard [38].

3.4.1 Evaluation of parabolic surface error

The experimental thermal efficiency of a PTC can be defined as the ratio of the heat received by the working fluid to the normal solar irradiance energy that is incident to the aperture [2, 31, 40-42]

$$\eta_c = \frac{\dot{m} \times C_p \times (T_{out} - T_{in})}{A_a \times I_b} \quad (6)$$

where (\dot{m}) is the water mass flow rate in the receiver tube, (C_p) is the specific heat capacity (J/kg, °C), (A_a) is the aperture area, (I_b) is the solar beam radiation (W/m^2), and (T_{out}), (T_{in}) is the outlet and inlet temperature of the receiver tube respectively.

In addition, the thermal efficiency of a PTC that is operating under steady state conditions may be defined as follows according to ASHRAE Standard 93 (1986) ASHRAE [29]:

$$\eta_c = F_R \eta_o - \frac{F_R U_L}{C} \left(\frac{T_{in} - T_{amb.}}{I_b} \right) \quad (7)$$

where ($F_R \eta_o$) is the intercept; ($\frac{F_R U_L}{C}$) is the slope; and (C) is the concentration ratio, which is defined as the rate of the collector aperture area (A_a) to the ratio of the receiver area (A_r). If the

collector thermal efficiency from Eq. (6) is plotted against $\left(\frac{T_{in}-T_{amb.}}{I_b}\right)$, then the result is a straight line. This result indicates that the overall heat coefficient (U_L) is constant and that the line equation represents collector thermal efficiency Jafar and Sivaraman [9], as shown in Figure 13.

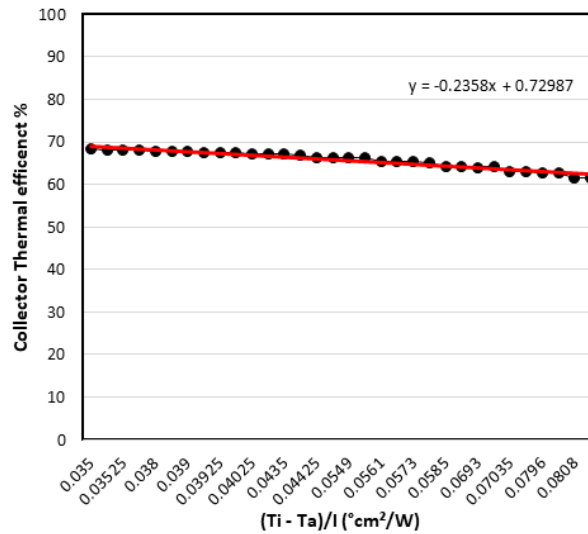


Fig. 13. Collector thermal efficiency curve

The curve equation shows that the slope is 0.2358 and the intercept is 0.72987. Therefore, the experimental thermal efficiency equation can be expressed as

$$\eta_c = 0.72987 - 0.2358 \left(\frac{T_{in}-T_{amb.}}{I_b} \right) \tag{8}$$

Then, the comparison between the collector thermal efficiency in the current work according to Eq. (8) and those in other studies [9, 11, 43, 46] is presented in Table 2.

Table 2
 Comparison of Collector Efficiency Equations

Efficiency Equation	References
$\eta_c = 0.6128 - 2.302 \left(\frac{T_{in} - T_{amb.}}{I_b} \right)$	Jaramillo <i>et al.</i> , [23]
$\eta_c = 0.65 - 0.382 \left(\frac{T_{in} - T_{amb.}}{I_b} \right)$	Arasu and Sornakumar [44]
$\eta_c = 0.642 - 0.441 \left(\frac{T_{in} - T_{amb.}}{I_b} \right)$	Kalogirou <i>et al.</i> , [45]
$\eta_c = 0.638 - 0.387 \left(\frac{T_{in} - T_{amb.}}{I_b} \right)$	Kalogirou [46]
$\eta_c = 0.6905 - 0.3865 \left(\frac{T_{in} - T_{amb.}}{I_b} \right)$	Valan and Sornakumar [11], Arasu and Sornakumar [44]
$\eta_c = 0.71 - 0.2454 \left(\frac{T_{in} - T_{amb.}}{I_b} \right)$	Jafar and Sivaraman [9]
$\eta_c = 0.72987 - 0.2358 \left(\frac{T_{in} - T_{amb.}}{I_b} \right)$	Current work

3.5 Theoretical Calculations

The thermal efficiency of the collector was theoretically calculated to validate the experimental result. One of the most important PTC performance parameters is optical efficiency, which is defined as the ratio of the energy absorbed by the receiver tube to the energy incident on the aperture of the concentrator. In mathematical of primary design of optical efficiency, the optical efficiency considered to be $\eta_o = 0.7$ at angle of incidence ($i = 0^\circ$) as commonly [12]. Optical efficiency depends on the optical properties of the involved materials and collector geometry. Optical efficiency can be expressed as Jaramillo *et al.*, [43]

$$\eta_o = \rho_m \cdot \tau_c \cdot \alpha_r \cdot \gamma \cdot [(1 - A_f \tan i) \cos i] \quad (9)$$

Where (i) is the angle of incidence that is represented by the angle between the radiation lines of the sun and the perpendicular aperture. Mirror reflectivity (ρ_m), receiver absorptivity (α_r), and cover material transmittance (τ_c) are recommended as (0.8), (0.9), and (0.95), respectively [17, 27-30]. The intercept factor (γ) is defined as the ratio of the energy intercepted by the receiver to the energy reflected by the focusing device. This factor depends on receiver size and solar beam diffusion. Guven and Bannerot (1985) developed the expression for evaluating the intercept factor as follows Güven and Bannerot [37]:

$$\gamma = \frac{1 + \cos \phi_r}{2 \sin \phi_r} \times \int_0^{\phi_r} \text{Erf} \left(\frac{\sin \phi_r (1 + \cos \phi) (1 - 2d^* \sin \phi) - \pi \beta^* (1 + \cos \phi_r)}{\sqrt{2\pi} \sigma^* (1 + \cos \phi_r)} \right) - \text{Erf} \left(\frac{\sin \phi_r (1 + \cos \phi) (1 + 2d^* \sin \phi) + \pi \beta^* (1 + \cos \phi_r)}{\sqrt{2\pi} \sigma^* (1 + \cos \phi_r)} \right) \frac{d\phi}{(1 + \cos \phi_r)} \quad (10)$$

where (ϕ_r) is the collector rim angle in rad; and (σ^*) is the universal random error parameter, which can be calculated as Güven and Bannerot [37]

$$\sigma^* = \sigma_{total} \cdot C \quad (\text{rad}), \quad (11)$$

Where the standard deviation of the total reflected energy distribution at normal incidence (σ_{total}) is estimated using Eq. (5). The concentration ratio (C) varies from low values less than the unity to high values of 10^5 [2, 51].

$$C = \frac{A_a}{A_r} = \frac{W_a \cdot L}{\pi \cdot D_o \cdot L} = \frac{W_a}{\pi \cdot D_o} \quad (12)$$

The symbol (d^*) in Eq. (10) is the universal nonrandom error parameter caused by receiver mislocation and reflector profile errors. This variable can be determined as follows Güven and Bannerot [19]:

$$(d^* = \frac{d_r}{D}) \quad (13)$$

Where (d_r), which represents receiver displacement from the focus of the parabola, is assumed to be 2 mm Valan and Sornakumar [11].

Moreover, (β^*) in Eq. (10) represents the universal nonrandom error parameter caused by angular errors; this variable can be determined as follows Güven and Bannerot [19, 37]:

The hour angle (ω) in Eqs. (17) and (18) (Figure 14) is recorded from solar noon, with positive afternoons and negative mornings. It is based on the nominal time of 24 h that is required for the sun to move 360° around the Earth or 15° per hour (e.g., if the calculations are performed 2 h before solar noon, then $\omega = 15^\circ \times 2 = -30^\circ$ (morning)) Braun and Mitchle [52].

The latitude angle (L) in Eq. (18) is the angle between the line from the centre of the Earth to the site and the equatorial plane. Latitude is considered negative south of the equator and positive north of the equator Braun and Mitchle [52].

From Eq. (15), the error of the tracking mechanism (surface slop β) is 0.2° and 0.16° at radiation levels of 1760.38 W/m^2 and 2130.6 W/m^2 , respectively, which were measured first on August 2017 in Baghdad, Iraq. Thus, the maximum (worst) error of the tracking mechanism is 0.2° .

The collector geometric factor (A_f) in Eq. (9) is the effective reduction of the aperture area due to abnormal incidence effects. This factor can be expressed as Jaramillo *et al.*, [43].

$$A_f = \frac{\frac{2}{3} W_a h_p + f W_a \left(1 + \frac{W_a^2}{48 f^2}\right)}{A_a} \quad (20)$$

A simple MATLAB program was developed to evaluate the intercept factor (γ). This program mainly computes the two error functions and uses the Simpson integration method (SIM) to numerically integrate the integral. SIM uses the one-degree steps of the rim angle (ϕ) (for $\phi = 1^\circ$ to $\phi_r = 90^\circ$). The calculated values are added and then divided by the number of steps to finally obtain the intercept factor value. The flowchart of the intercept factor program is shown in Figure 15.

The Angle of Incidence (i) in Eq. (9) is the angle between the radiation lines of the sun and the perpendicular aperture. It is measured between a sun's ray and the surface normal Braun and Mitchle [52].

$$\cos i = \cos \theta_z \cos \beta + \sin \theta_z \sin \beta \cos(a_s - a) \quad (21)$$

The theoretical test involves calculating the heat removal factor (F_R), which was presented by Kalogirou (2009). It represents the ratio of the actual useful energy gain that would result if the collector-absorbing surface had been at the local fluid temperature Kalogirou [54-55].

$$F_R = \frac{\dot{m} c_p}{A_r U_L} \left(1 - \text{Exp} \left[-\frac{U_L \hat{F} A_r}{\dot{m} c_p} \right]\right) \quad (22)$$

Where (\hat{F}) is the collector efficiency factor, which was presented by Kalogirou (2009) as follows Kalogirou [54-55]:

$$\hat{F} = \frac{\frac{1}{U_L}}{\frac{1}{U_L} + \frac{D_o}{h \cdot D_i} + \left(\frac{D_o}{2 k_f} \ln \frac{D_o}{D_i}\right)} \quad (23)$$

where (h) is the convection heat transfer coefficient (W/m. $^\circ\text{C}$), (k_f) is the working fluid thermal conductivity (W/m. $^\circ\text{C}$), and (U_L) is the thermal loss coefficient of the parabolic collector. (U_L) depends on the magnitude of conductive, radiative, and convective losses, which in turn, depend on the operating temperature of the collector that is relative to the environment. The thermal loss coefficient can be expressed as [56-57].

$$U_L = \frac{Q}{\pi D_o L (T_m - T_{amb.})} \quad (24)$$

where (Q) is the receiver heat transfer rate, (T_a) is ambient temperature, and (T_m) is the mean receiver surface temperature.

Thus, the theoretical intercept test ($F_R \eta_o$) and slope ($\frac{F_R U_L}{C}$) are calculated as 0.77947 and 0.2257, respectively, by applying Eq. (9) and Eqs. (22) to (24). Table 3 presents the comparison between the theoretical calculations of the intercept and slope and the experimental values.

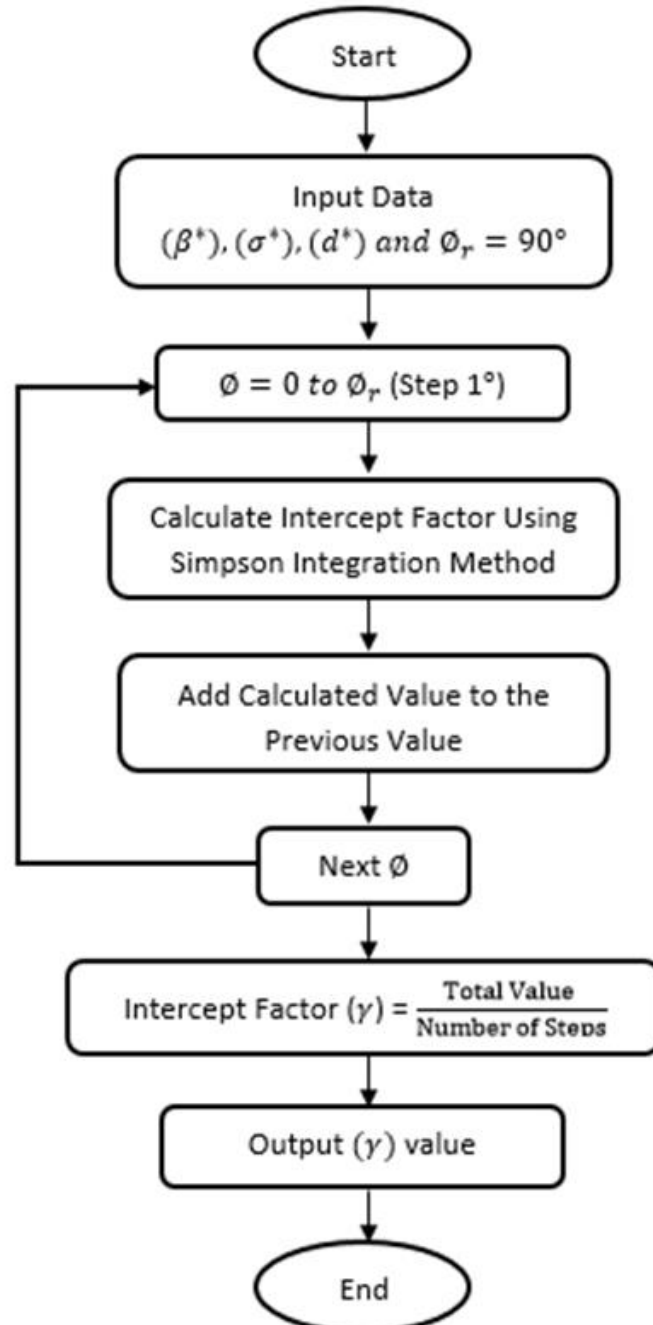


Fig. 15. Intercept factor program flow chart

Table 3

Collector Performance comparison

Item	Test Intercept ($F_R \eta_o$)	Test Slope ($\frac{F_R U_L}{C}$)
Theoretical Performance (Current Work)	0.77947	0.2257
Experimental Performance (Current Work)	0.72987	0.2358
% Difference	6.36	4.28

The comparison in Table 3, indicates a reasonable difference between the experimental and theoretical results, which further indicates that the newly designed and developed stainless steel PTC is accurately built.

3.6 Collector Time Constant Test

The collector time constant is the time required for the fluid that is leaving the collector to reach 63.2% of its ultimate steady state value after a step change in incident radiation. In accordance with the ASHRAE standard, the collector time constant is the time required to change the quantity in Eq. (25) from 1.0 to 0.368 [29, 44].

$$\left(\frac{T_{(out)f} - T_{out(t)}}{T_{(out)f} - T_{in}} \right) \tag{25}$$

Where $(T_{(out)f})$ is the final outlet temperature of the collector fluid, and $(T_{out(t)})$ is the outlet temperature of the collector fluid after time (t) .

The PTC time constant should be determined to evaluate the transient behaviour of the collector and select a suitable time for the steady state or quasi-steady state efficiency tests Jaramillo *et al.*, [43]. To determine the time constant, a test was conducted directly after running the device, during which the collector was initially at the defocused position. Then, the collector moved to the focused position, and measurements were recorded every 10 s until steady state conditions were achieved. In the test, the water inlet temperature of the collector was maintained at ambient temperature. The time constant of the collector was determined as 75 s, as shown in Figure 16.

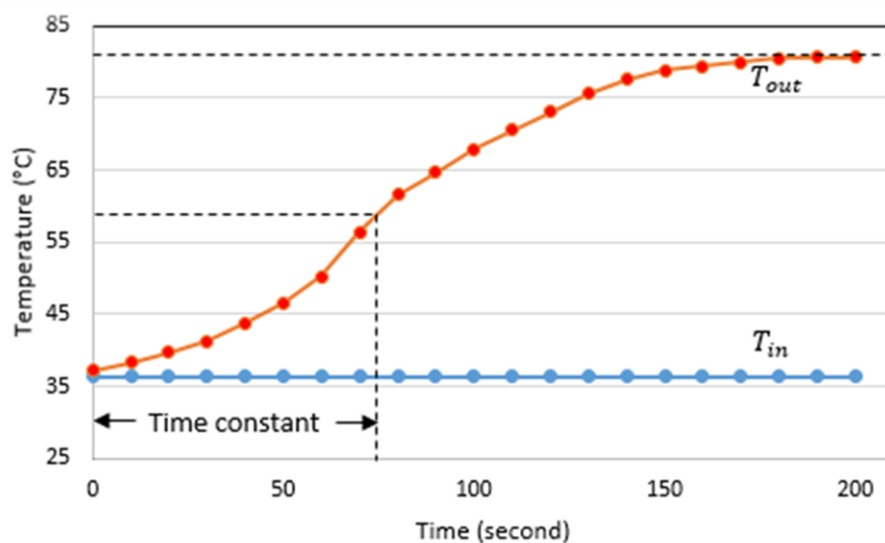


Fig. 16. Collector time constant

3.7 PTC Evaluations

The collector unit includes a reflective surface of the trough, receiver system, a storage tank, and manual tracking system as shown in Figure 17. The PTC collector installed at an open area of the solar energy on the roof of the house in Baghdad-Iraq (latitude 33.2° N) with strong sunshine insolation varied between ($1600\text{-}2200\text{ W/m}^2$) and the mean ambient temperature varied between ($36\text{-}53^\circ\text{C}$). The maximum temperature of water production when PTC running was 129°C for close system and 92°C for open system.

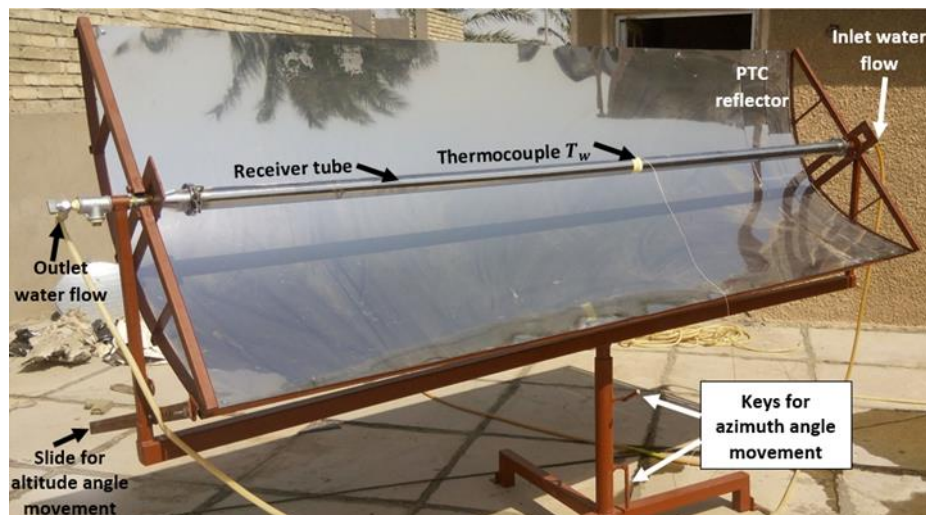


Fig. 17. Parabolic trough collector

4. Conclusions

The design, fabrication, and testing of a 90° rim angle medium-scale stainless steel parabolic trough for a solar-powered PTC is presented in this study according to ASHRAE Standard 93 (1986). Theoretical calculations and primary design were achieved with all possible evaluations that provide accuracy design. The experimental results show that the maximum water obtained from system is more than 226 L/day with temperature $\geq 50^\circ\text{C}$ at flow rate of 0.00925 kg/s , and at mentioned flow rate is 92°C . The deviation at the parabola center is measured using a dial gauge. The maximum deflection of parabolic trough was obtained when loads are applied to represent wind force that corresponds to a wind velocity of 34 m/s is only 0.85 mm, which is considered suitable. The 50 mm diameter receiver tube of a 56.4 mm wide solar image in the focal plane showed a maximum deformation of 1.43 mm, which is within acceptable limits. The thermal performance test of the new PTC that was modelled and developed for hot water generation is achieved. The standard deviation of the distribution of parabolic surface errors is determined as 0.009165 rad from the collector performance test according to ASHRAE Standard 93 (1986), which indicates that the surface is accurately built. In the experimental test, a slope and test intercept of 0.2358 and 0.72987, respectively, are derived. The collector efficiency equation is comparable with those in other reported works and demonstrated improved collector efficiency. The maximum error of the tracking mechanism is $\pm 0.2^\circ$. The theoretically calculated slope and intercept values are compared with the experimental results. The comparison indicates 4.28% and 6.36% differences among slopes and intercepts, respectively, which further show that the design steps followed in the current work are correct. The time constant for the new PTC is estimated as 75 s, which implies fast collector response for maintaining quasi-steady state conditions. The theoretical intercept test and slope are calculated

as 0.77947 and 0.2257, respectively. The comparison between the theoretical calculations of the intercept and slope and the experimental values indicates a reasonable difference between the two results, which further indicates that the newly designed and developed stainless steel PTC is accurately built.

Acknowledgement

The financial support by Putra grant for post graduate (IPS) is highly acknowledged

References

- [1] Abdulhamed AJ, Adam NM, Hairuddin AA, Hanaa KA. "Design and fabrication of a heat exchanger for portable solar water distiller system." *International Food Research Journal* 23 (2016): 15–22.
- [2] Abdulhamed AJ, Adam NM, Ab-Kadir MZA, Hairuddin AA. "Review of solar parabolic-trough collector geometrical and thermal analyses, performance, and applications." *Renewable and Sustainable Energy Review* 91 (2018): 822–831.
- [3] Shahin SM, Orhan MF, Uygul F. "Thermodynamic analysis of parabolic trough and heliostat field solar collectors integrated with a Rankine cycle for cogeneration of electricity and heat." *Solar Energy* 136 (2016): 183–196.
- [4] Kalogirou SA. "Use of solar parabolic trough collectors for hot water production in Cyprus. A feasibility study." *Renewable Energy* 2, no. 2 (1992): 117–124.
- [5] Abdulhamed AJ, Adam NM, Hairuddin AA, Alsabahi HK. "Effect of Tube thickness for shell and tube heat exchanger in portable solar water distiller." *International Journal of Engineering Research & Technology* 4, no. 11 (2015): 37–42.
- [6] Thomas A. "Solar steam generating systems using parabolic trough concentrators." *Energy Conversion and Management* 37, no. 2 (1996): 215–245.
- [7] Alhamdo, M. H., and A. J. Alkhakani. "Dynamic response of a modified water tank exposed to concentrated solar energy." In *IOP Conference Series: Materials Science and Engineering*, vol. 227, no. 1, p. 012002. IOP Publishing, 2017.
- [8] Fernández-García A, Zarza E, Valenzuela L, Pérez M. "Parabolic-trough solar collectors and their applications." *Renewable and Sustainable Energy Review* 14, no. 7 (2010): 1695–1721.
- [9] Jafar KS, Sivaraman B. "Performance characteristics of parabolic solar collector water heater system fitted with nail twisted tapes absorber." *Journal of Engineering Science and Technology* 12, no. 3 (2017): 608-621.
- [10] Jaramillo OA, Borunda M, Velazquez-Lucho KM, Robles M. "Parabolic trough solar collector for low enthalpy processes: An analysis of the efficiency enhancement by using twisted tape inserts." *Renewable Energy* 93 (2016): 125–141.
- [11] Valan AA, Sornakumar T. "Design, manufacture and testing of fiberglass reinforced parabola trough for parabolic trough solar collectors." *Solar Energy* 81, no. 10 (2007): 1273–1279.
- [12] Jaramillo OA, Venegas-Reyes E, Aguilar JO, Castrejón-García R. "Parabolic trough concentrators for low enthalpy processes." *Renewable and Sustainable Energy Review* 60 (2013): 529-539.
- [13] Fuqiang W, Ziming C, Jianyu T, Yuan Y. "Progress in concentrated solar power technology with parabolic trough collector system: A comprehensive review." *Renewable and Sustainable Energy Review* 79 (2017): 1314-1328.
- [14] Bellos E, Tzivanidis C. "Investigation of a star flow insert in a parabolic trough solar collector." *Applied Energy* 224 (2018): 86-102.
- [15] Fuqiang W, Zhexiang T, Xiangtao G, Jianyu T. "Heat transfer performance enhancement and thermal strain restraint of tube receiver for parabolic trough solar collector by using asymmetric outward convex corrugated tube." *Energy* 114 (2016): 275-292.
- [16] Fuqiang W, Qingzhi L, Huaizhi H, Jianyu T. "Parabolic trough receiver with corrugated tube for improving heat transfer and thermal deformation characteristics." *Applied Energy* 146 (2016): 411-424.
- [17] Bellos E., C. Tzivanidis, K. A. Antonopoulos, and G. Gkinis. "Thermal enhancement of solar parabolic trough collectors by using nanofluids and converging-diverging absorber tube." *Renewable Energy* 94 (2016): 213-222.
- [18] Huang, Zhen, Zeng-Yao Li, Guang-Lei Yu, and Wen-Quan Tao. "Numerical investigations on fully-developed mixed turbulent convection in dimpled parabolic trough receiver tubes." *Applied Thermal Engineering* 114 (2017): 1287-1299.
- [19] Cheng, Z. D., Y. L. He, and F. Q. Cui. "Numerical study of heat transfer enhancement by unilateral longitudinal vortex generators inside parabolic trough solar receivers." *International journal of heat and mass transfer* 55, no. 21-22 (2012): 5631-5641.

- [20] Muñoz J, Abánades A. "Analysis of internal helically finned tubes for parabolic trough design by CFD tools Javier." *Applied Energy* 88, no.11 (2011): 4139-4149.
- [21] Wang P, Liu DY, Xu C. "Numerical study of heat transfer enhancement in the receiver tube of direct steam generation with parabolic trough by inserting metal foams." *Applied Energy* 102 (2013): 449-460.
- [22] Reddy KS, Ravi Kumar K, Ajay CS. "Experimental investigation of porous disc enhanced receiver for solar parabolic trough collector." *Renewable Energy* 77 (2015): 308-319.
- [23] Gong, Xiangtao, Fuqiang Wang, Haiyan Wang, Jianyu Tan, Qingzhi Lai, and Huaizhi Han. "Heat transfer enhancement analysis of tube receiver for parabolic trough solar collector with pin fin arrays inserting." *Solar Energy* 144 (2017): 185-202.
- [24] Liu, Peng, Nianben Zheng, Zhichun Liu, and Wei Liu. "Thermal-hydraulic performance and entropy generation analysis of a parabolic trough receiver with conical strip inserts." *Energy conversion and management* 179 (2019): 30-45.
- [25] Song, Xingwang, Guobo Dong, Fangyuan Gao, Xungang Diao, Liqing Zheng, and Fuyun Zhou. "A numerical study of parabolic trough receiver with nonuniform heat flux and helical screw-tape inserts." *Energy* 77 (2014): 771-782.
- [26] Mwesigye, Aggrey, Tunde Bello-Ochende, and Josua P. Meyer. "Heat transfer and entropy generation in a parabolic trough receiver with wall-detached twisted tape inserts." *International Journal of Thermal Sciences* 99 (2016): 238-257.
- [27] Demagh, Yassine, Ahmed A. Hachicha, Hocine Benmoussa, and Yassine Kabar. "Numerical investigation of a novel sinusoidal tube receiver for parabolic trough technology." *Applied Energy* 218 (2018): 494-510.
- [28] Bellos, Evangelos, and Christos Tzivanidis. "Alternative designs of parabolic trough solar collectors." *Progress in Energy and Combustion Science* 71 (2019): 81-117.
- [29] ASHRAE Standard. *Method of testing to determine the thermal performance of solar collectors*. American Society of Heating, Refrigerating and Air – Conditioning Engineers. Atlanta, GA. ASHRAE Standard 93. 1986.
- [30] García-Cortés S, Bello-García A, Ordóñez C. "Estimating intercept factor of a parabolic solar trough collector with new supporting structure using off-the-shelf photogrammetric equipment." *Applied Energy* 92 (2012): 815–821.
- [31] Menbari A, Alemrajabi AA, Rezaei A. "Experimental investigation of thermal performance for direct absorption solar parabolic trough collector (DASPTC) based on binary nanofluids." *Experimental Thermal and Fluid Science* 80 (2017): 218–227.
- [32] Kasaeian A, Daviran S, Azarian RD, Rashidi A. "Performance evaluation and nanofluid using capability study of a solar parabolic trough collector." *Energy Conversion and Management* 89 (2015): 368–375.
- [33] Shankar GN, Srinivas T. "Design and modeling of low temperature solar thermal power station." *Applied Energy* 91, no. 1 (2012): 180–186.
- [34] Abdulhamed AJ, Adam NM, Ab-kadir MZ, Hairuddin AA. "Flow and Thermal Mechanisms in Receiver Tube of Parabolic Trough Collectors with Rings Axially Connected Together and Radially Connected to the Inner Tube Surface." *Journal of Engineering and applied science* 15, no.3 (2020): 762-772.
- [35] Behar O, Khellaf A, Mohammadi K. "A novel parabolic trough solar collector model - Validation with experimental data and comparison to Engineering Equation Solver (EES)." *Energy Conversion and Management* 106 (2015): 268–281.
- [36] Rabl A. "Comparison of solar concentrators." *Solar Energy* 18, no. 2 (1976): 93–111.
- [37] Güven HM, Bannerot RB. "Derivation of universal error parameters for comprehensive optical analysis of parabolic." *Journal of Solar Energy Engineering* 108, no. 4 (1986): 275–281.
- [38] Güven HM, Bannerot RB. "Determination of error tolerances for the optical design of parabolic troughs for developing countries." *Solar Energy* 36, no. 6 (1986): 535–550.
- [39] Treadwell GW. "Design considerations for parabolic-cylindrical solar collectors." *International Solar Energy Society* 2 (1976): 235–252.
- [40] Gaul H, Rabl A. "Incidence-angle modifier and average optical efficiency of parabolic trough collectors." *Journal of Solar Energy Engineering* 102, no. 1 (1980): 16–21.
- [41] Ghasaq Adheed Hashim, Nor Azwadi Che Sidik. "Numerical study of harvesting solar energy from small-scale asphalt solar collector." *Journal of Advanced Research Design* 2, no. 1 (2014): 10-19.
- [42] Amira L, Suhaimi M, Noreffendy T, Mohd A, Fadhil A. "Numerical Analysis of Solar Hybrid Photovoltaic Thermal Air Collector Simulation by ANSYS." *CFD Letters* 11, no.2 (2019): 1-11.
- [43] Jaramillo, O. A., E. Venegas-Reyes, J. O. Aguilar, R. Castrejón-García, and F. Sosa-Montemayor. "Parabolic trough concentrators for low enthalpy processes." *Renewable energy* 60 (2013): 529-539.
- [44] Arasu, A. Valan, and T. Sornakumar. "Performance Characteristics of ParabolicTrough Solar Collector System for Hot Water Generation." *International Energy Journal* 7, no. 2 (2006): 137-145.
- [45] Kalogirou, Soteris A., S. Lloyd, J. Ward, and P. Eleftheriou. "Design and performance characteristics of a parabolic-trough solar-collector system." *Applied energy* 47, no. 4 (1994): 341-354.

- [46] Kalogirou, Soteris. "Parabolic trough collector system for low temperature steam generation: design and performance characteristics." *Applied Energy* 55, no. 1 (1996): 1-19.
- [47] Theunissen, P-H., and W. A. Beckman. "Solar transmittance characteristics of evacuated tubular collectors with diffuse back reflectors." *Solar energy* 35, no. 4 (1985): 311-320.
- [48] Amina, Benabderrahmane, Aminallah Miloud, Laouedj Samir, Benazza Abdelylah, and J. P. Solano. "Heat transfer enhancement in a parabolic trough solar receiver using longitudinal fins and nanofluids." *Journal of Thermal Science* 25, no. 5 (2016): 410-417.
- [49] Tesfamichael, T., and E. Wäckelgård. "Angular solar absorptance and incident angle modifier of selective absorbers for solar thermal collectors." *Solar Energy* 68, no. 4 (2000): 335-341.
- [50] Herrick CS. "Optical transmittance measurements on a solar collector cover of cylindrical glass tubes." *Solar Energy* 28, no. 1 (1982): 5-11.
- [51] Good P, Ambrosetti G, Pedretti A, Steinfeld A. "A 1.2MWth solar parabolic trough system based on air as heat transfer fluid at 500°C — Engineering design, modelling, construction, and testing." *Solar Energy* 139 (2016): 398-411.
- [52] Braun JE, Mitchle JC. "Solar geometry for fixed and tracking surfaces." *Solar Energy* 31, no. 5 (1983): 439-444.
- [53] Cooper, P. I. "The absorption of radiation in solar stills." *Solar energy* 12, no. 3 (1969): 333-346.
- [54] Kalogirou, Soteris A. "A detailed thermal model of a parabolic trough collector receiver." *Energy* 48, no. 1 (2012): 298-306.
- [55] Sachit, Fadhil Abdulameer, Mohd Afzanizam Mohd Rosli, Noreffendy Tamaldin, Suhaimi Misha, and Amira Lateef Abdullah. "Modelling, Validation and Analyzing Performance of Serpentine-Direct PV/T Solar Collector Design." *CFD Letters* 11 (2019): 50-65.
- [56] Ananth J, Jaisankar S. "Experimental studies on heat transfer and friction factor characteristics of thermosyphon solar water heating system fitted with regularly spaced twisted tape with rod and spacer." *Energy Conversion and Management* 73 (2013): 207-213.
- [57] Arasu, A. Valan, and T. Sornakumar. "Design and simulation analysis of a parabolic trough solar collector hot water generation system." *International Energy Journal* 6, no. 2 (2005): 13-25.